Frequency Dependent Characteristics of Radiation from a Voltage Source on a Covered Microstrip Line

William L. Langston, Jeffery T. Williams, and David R. Jackson

Department of Electrical and Computer Engineering,
University of Houston, Houston, Texas, 77204-4005, USA

Francisco Mesa

Department of Applied Physics 1,
University of Seville, Seville, 41012, Spain

Abstract — **The fields radiated from the currents induced on a covered microstrip transmission line by a finite-gap voltage source are presented. The character of these radiated fields has been examined in detail as the frequency is varied. It is shown that there is a smooth transition in the total radiation field from the spectral-gap region at lower frequencies to higher frequencies where a physical leaky mode exists. A characteristic leakage beam develops gradually as the frequency increases. When the leakage beam first develops, the observed radiation angle is greater than that predicted by the leaky mode alone. Crosstalk radiation can be significant even before the leaky mode becomes physical.**

I. INTRODUCTION

The existence of dominant (quasi-TEM) leaky modes on printed-circuit transmission lines has been the subject of considerable interest. These modes are usually undesirable since they result in increased attenuation of the signal, and can result in crosstalk with adjacent circuit components and interference with bound modes that also propagate on the line. Leaky dominant modes have been found on a number of planar transmission line structures including multilayer stripline structures and microstrip lines with isotropic and anisotropic substrates.

Recently, the current on multilayer stripline [1] and covered microstrip [2] structures due to an excitation from a small, finite-length gap feed on the line was studied. It was shown that the total current on the strip excited by the source can be decomposed into the sum of the well-known bound-mode current and a continuous-spectrum current. It was demonstrated that spurious transmission effects can result due to the interference of the bound-mode and the continuous-spectrum currents, particularly when a physical leaky mode is present.

In this summary, the calculation of the *fields* radiated by the bound-mode and continuous-spectrum currents excited by a finite source on covered microstrip transmission lines will be presented. The characteristics of the radiated fields will be studied in detail for frequencies extending over a wide range, including: (a) where no leaky mode exists; (b) where a leaky mode exists, but is nonphysical (inside the spectral-gap region); and (c) where a physical leaky mode exists (one which is fast with respect to the dominant parallel-plate mode of the structure). The purpose of the study is to examine, for the first time, how the radiated fields evolve with frequency throughout the spectral-gap region. Important insight is obtained as to when crosstalk from radiation at discontinuities is significant in microwave integrated circuits.

II. SUMMARY OF ANALYSIS

A diagram of the covered microstrip structure (two-layer stripline) with a small, but finite 1-V gap source is shown in Fig. 1. The conducting strip is assumed to be infinite in the $\pm z$ directions and all of the conductors are assumed to be perfect conductors. For simplicity, the strip width W is assumed to be small so that the transverse component of the current can be neglected. Therefore, the current density along the strip is given by

$$J_z(x,z) = I(z)\eta(x), \qquad (1)$$

where $\eta(x)$ is the normalized transverse shape function for the strip current $I(z)$. A closed-form solution for the Fourier transform of the strip current is obtained by applying the Galerkin method in the spectral domain. The total strip current is then expressed as [1]

0-7803-7239-5/02/$10.00 © 2002 IEEE

$$I(z) = \frac{1}{2\pi} \int_{C_z} \tilde{I}(k_z) e^{-jk_z z} dk_z \,, \tag{2}$$

where C_z is a Sommerfeld-type path in the complex k_z plane (one that is deformed around poles and branch points) [1]. From the Galerkin solution procedure, the transform of the strip current is given by

$$\tilde{I}(k_z) = \frac{2\pi \tilde{E}_{GAP}(k_z)}{\int_{C_x} \tilde{G}_{ZZ}(k_x, k_z, h) \tilde{\eta}^2(k_x) dk_x} \,, \tag{3}$$

where $\tilde{E}_{GAP}$ is the Fourier transform of the impressed electric field of the gap source, $\tilde{G}_{ZZ}$ is the $\hat{\mathbf{z}}\hat{\mathbf{z}}$ component of the spectral-domain dyadic electric-field Green's function at $y = h$, and $\tilde{\eta}$ is the Fourier transform of the transverse profile of the strip current density.

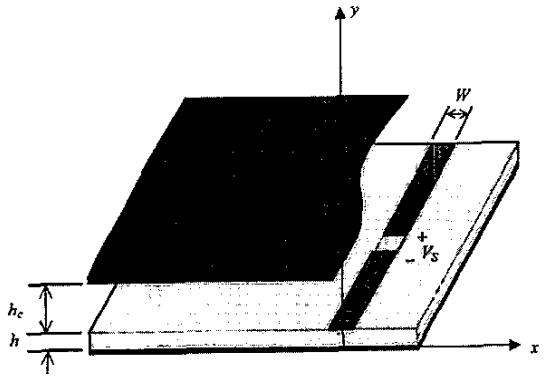

Fig. 1. Covered microstrip structure with a small, finite-length 1-V gap source (V_s = 1 V).

The total current (2) can be decomposed by suitably deforming the path of integration in the k_z plane [1]. If the original path is deformed around the branch cut, the total current is expressed as the sum of a residue contribution from a captured bound mode (BM) pole – the bound-mode current – and the contribution from the integral around the branch cuts in the lower half plane – the continuous-spectrum current. The continuous-spectrum current can be further resolved into one or more physical leaky-mode currents and a "residual-wave" current by deforming to a steepest-descent path [3].

Once determined, the strip current is used to find the fields radiated by the line and feed. Assuming that only the TM_0 parallel-plate mode is above cutoff in the background structure, the TM_0 parallel-plate mode field radiated by the strip current is directly calculated by starting with the parallel-plate mode field radiated by a *z*-directed infinitesimal electric dipole, and then integrating over the strip current [2]. The results are put in a convenient normalized form by calculating the substrate voltage V_h, which is defined as the vertical integral in *z* of the radiated parallel-plate mode electric field in the substrate from *0* to *h*.

III. RESULTS

In this summary, a covered microstrip with $h_c = h = W$ and a substrate relative permittivity of ε_r = 2.2 is examined. A dispersion plot for this structure is shown in Fig. 2.

Figures 3-7 show the substrate voltage in a region near the source, for frequencies spanning the entire range of Fig. 2. At lower frequencies, the radiated field is weak and is predominately due to radiation from the discontinuity in the bound-mode current at the source (a bound-mode source-discontinuity radiation) as shown in Fig. 3. Figure 4 shows the low frequency case $h = 0.0205\lambda_0$. This particular frequency lies at the beginning of the leaky-mode region in Fig. 2, where two improper-real modes have merged to form a complex leaky mode. The leaky mode is nonphysical at this frequency. The total radiation field is comprised mainly of a bound-mode radiation field with only a small contribution from the continuous-spectrum radiation field. Hence, we can see characteristics typical of a bound-mode radiation field, including an interference pattern along the length of the line that is caused by the interference between a bound-mode source-discontinuity radiation field and a transversely decaying field that corresponds to the field of the bound mode on an infinite line [2].

As the frequency increases throughout the spectral-gap region ($h < 0.05\lambda_0$), the radiation field is increasing in magnitude rapidly and changing character, as a leakage beam begins to evolve. This change in character occurs because the continuous-spectrum radiation field is becoming more significant relative to the bound-mode radiation field, and because the continuous-spectrum radiation field is becoming more closely approximated by the field of the leaky mode. Once the frequency is increased to the end of the spectral gap at $h = 0.05\lambda_0$, it is found from Fig. 5 that the overall field magnitude has nearly doubled from the level at the onset of leakage, and there is now a noticeable beam of leakage away from the line ($\phi \approx 17°$). However, the beam is not very well defined.

The change in character of the total radiation field due to the strengthening of the continuous-spectrum field allows the field transition into the physical leaky-mode region to be continuous. As the frequency is increased

beyond $h = 0.05\lambda_0$, the leaky-mode becomes physical, and the continuous-spectrum field (not shown here) begins to develop a characteristic leakage shape. This in turn influences the total radiation field. Hence, for $h = 0.07\lambda_0$ (shown in Fig. 6), there is a fairly well-defined angle of leakage away from the line ($\phi \approx 20^\circ$). This angle of leakage for the total radiation field is close to the predicted leakage angle based on the phase constant of the leaky mode,

$$\phi_0 = \cos^{-1}\left(\beta_z / \sqrt{\beta_z^2 + \beta_x^2}\right), \qquad (4)$$

which yields 17.2°.

The radiation field from the leaky-mode current alone for this case is shown in Fig. 7. The beam angle of this leaky-mode field, from Fig. 7, is approximately 13°. The reason the beam angle for the leaky-mode field is different from that predicted by the leaky-mode phase constant is that the leaky-mode current excited by the source is a bi-directional wave, which exhibits source-discontinuity radiation.

The reason that the beam angle for the total radiation field is much larger than that for the leaky mode field is that there is significant radiation from the bound-mode and residual-wave currents, which alters the shape of the total field.

The final frequency shown is $h = 0.1\lambda_0$ in Fig. 8. At this frequency the leaky mode is well within the physical region. The beam angle for the total radiation field is at about $\phi \approx 22^\circ$. This angle is fairly close to the predicted leakage angle based on the phase constant of the leaky mode ($\phi_0 \approx 22.2^\circ$). Figure 9 shows the radiation field of the leaky mode for this case. The actual leakage angle of the leaky-mode radiation field from Fig. 9 is about 19°, which matches well with the predicted leakage angle based on the phase constant. Furthermore, the actual leakage angle of the leaky-mode radiation field matches quite well with the beam angle for the total radiation field. This is a consequence of the fact that the radiation from the continuous-spectrum current is now significantly stronger than the bound-mode source-discontinuity radiation, and the fact that the continuous-spectrum current is dominated by the leaky-mode current.

In the case presented here, the field transition through the spectral-gap region is fairly smooth, since the attenuation constant of the leaky mode is relatively large (e.g., $\alpha / k_0 = 0.0832$ at $h = 0.07\lambda_0$). Results will be presented for other cases where the attenuation constant is smaller. Results will also be presented for the power launched into the bound-mode and the radiated power at different frequencies, to show how the radiated power increases significantly with frequency, resulting in a significant power loss in the circuit and a low bound-mode launching efficiency.

REFERENCES

[1] C. DiNallo, F. Mesa, and D. R. Jackson, "Excitation of leaky modes on multiplayer stripline structure," *IEEE Trans. Microwave Theory Tech.*, vol. 46, no. 8, pp. 1062-1071, Aug. 1998.

[2] W. L. Langston, J. T. Williams, D. R. Jackson, and F. Mesa, "Spurious radiation from a practical source on a covered microstrip line," *IEEE Trans. Microwave Theory Tech.*, vol. 49, no. 12, Dec. 2001.

[3] D. R. Jackson, F. Mesa, M. Freire, D. P. Nyquist, and C. Di Nallo, "An excitation theory for bound modes, leaky modes, and residual-wave current on stripline structures," *Radio Science*, vol. 35, no. 2, pp. 495-510, March-April 2000.

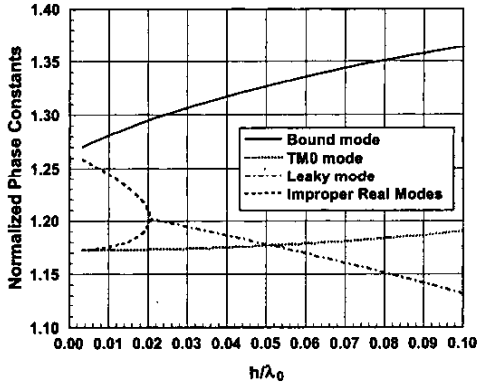

Fig. 2. Dispersion plot showing the normalized phase constants β/k_0 versus normalized frequency h/λ_0 for a covered microstrip ($h_c = h$, $W = h$, $\varepsilon_r = 2.2$).

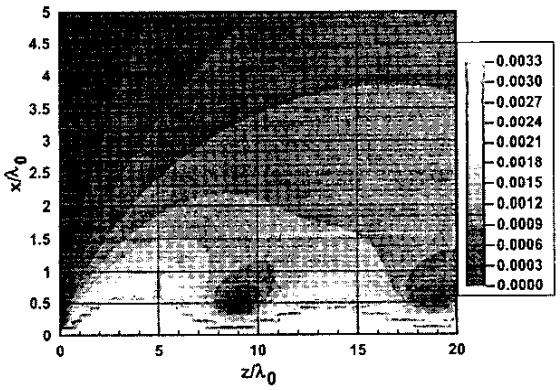

Fig. 3. Total substrate voltage for $h = 0.003\lambda_0$.

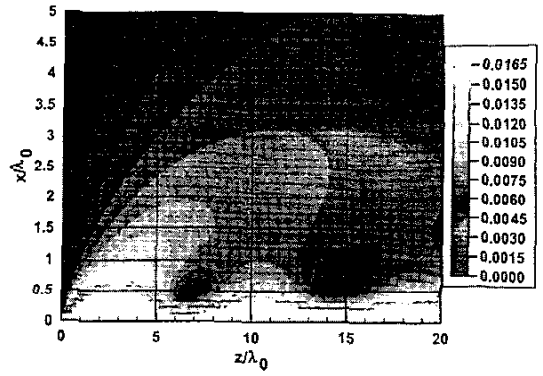

Fig. 4. Total substrate voltage for $h = 0.0205\lambda_0$.

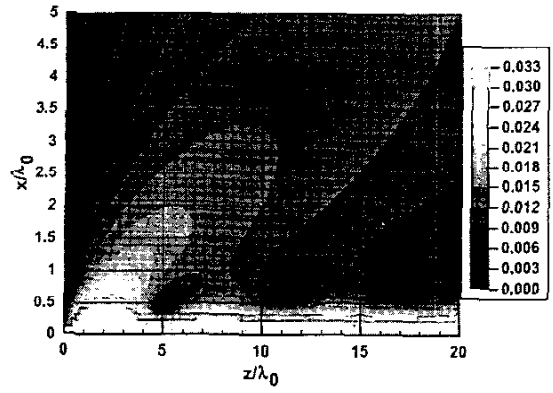

Fig. 5. Total substrate voltage for $h = 0.05\lambda_0$.

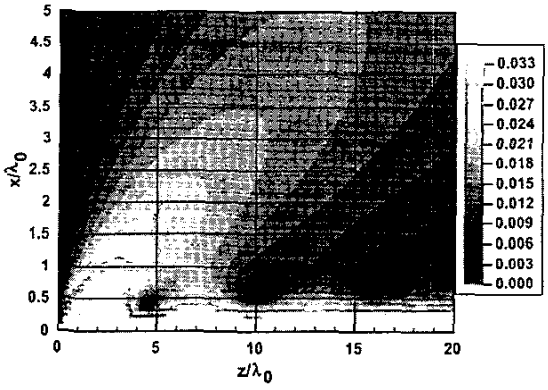

Fig. 6. Total substrate voltage for $h = 0.07\lambda_0$.

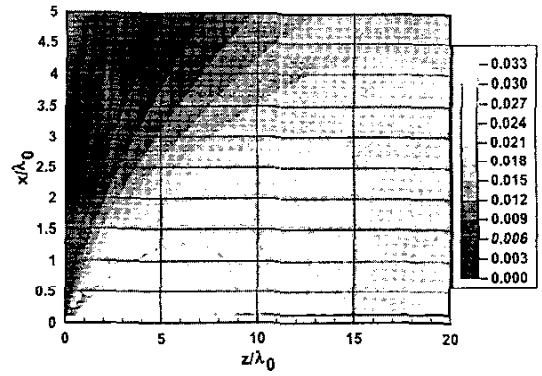

Fig. 7. Leaky mode substrate voltage for $h = 0.07\lambda_0$.

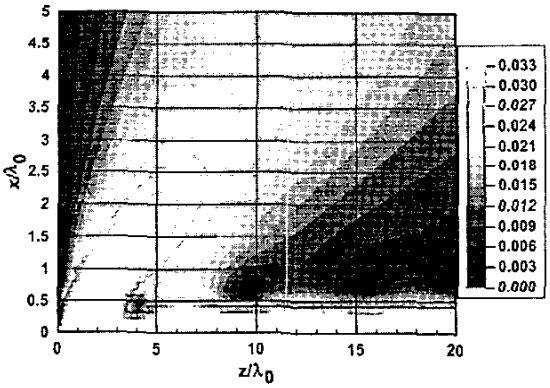

Fig. 8. Total substrate voltage for $h = 0.1\lambda_0$.

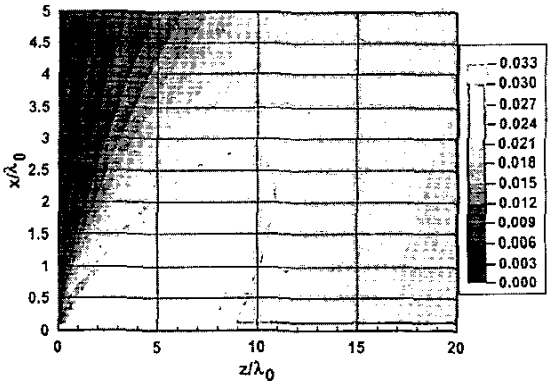

Fig. 9. Leaky mode substrate voltage for $h = 0.1\lambda_0$.